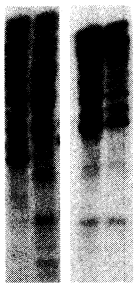

Fig. 5. Southern blot of susceptible (S) and resistant (R) strain individuals showing multicopy occurrence of Hel-1. Genomic DNA was digested with Apa LI, electrophoresed in a 0.8% agarose gel, blotted to nylon membranes, and probed with radiolabeled Hel-1 LTR.

volved in cell adhesion (*14*). Whatever its function, it is not essential for life, because YHD2 is viable and fertile under laboratory conditions despite being a "natural knockout" for HevCaLP. Whether its absence confers a fitness disadvantage in the field has important implications for resistance management, and this question can now be addressed with the information developed here.

These results suggest a new interpretation of our previous estimate of 0.0015 for the frequency of YHD2-type resistance alleles in field populations of *H. virescens* before widespread planting of Bt cotton (*15*). In that study, field-caught males were individually mated to homozygous resistant YHD2 virgin females, and their progeny were tested at a discriminating dose of Cry1Ac-containing diet. The majority of males were homozygous susceptible, as expected, producing only heterozygous progeny that did not grow on Cry1Ac because the resistance-conferring effect of *r1* is recessive. However, 3 of 1025 males were heterozygous, producing some progeny that did grow on the Cry1Ac diet because they inherited the *r1* allele from their YHD2 mother and a field-derived resistance allele from their father.

Our previous interpretation implicitly assumed that the paternally contributed resistance allele was also *r1*. But it is now evident that any other allele with a molecular lesion somewhere in HevCaLP preventing it from functioning as a lethal target would give the same result, because *r1* is a null allele. Thus, 0.0015 actually represents a frequency estimate of the entire class of such defective HevCaLP alleles. This statement applies even if *r1* itself does not occur in the field but arose in the lab. Thus, the development of efficient DNA-based methods to detect other types of mutants at *BtR-4* should be a high priority. Screening solely for the Hel-1 insert detects *r1* but may underestimate the total frequency of resistance alleles in the field.

Monitoring resistance allele frequencies in field populations will enable a direct test of whether the high-dose/refuge strategy is succeeding. If it starts to fail, detection of increasing heterozygote frequencies will indicate that a problem is looming, well before resistant homozygotes become frequent enough to cause uncontrollable outbreaks. This may allow enough time for the strategy to be adjusted to reverse the increase. We thus suggest that allele frequency monitoring be incorporated into resistance risk assessment. At the very least, preservation of DNA samples should accompany existing bioassay-based monitoring programs. Even if other Bt resistance genes are later discovered in *H. virescens*, any delay in initiating *BtR-4* allele monitoring erodes the opportunity to make informed modifications to a strategy that could sustain the use of Bt transgenics and prolong their environmental benefits of reducing dependency on conventional insecticides.

References and Notes

1. U.S. Environmental Protection Agency, *The Environmental Protection Agency's White Paper on Bt Plant-Pesticide Resistance Management* (EPA Publication 739-S-98-001, 1998; www.epa.gov/pesticides/biopesticides/white_bt.pdf).
2. F. Gould, A. Anderson, A. Reynolds, L. Bumgarner, W. Moar, *J. Econ. Entomol.* **88**, 1545 (1995).
3. D. G. Heckel, L. J. Gahan, F. Gould, A. Anderson, *J. Econ. Entomol.* **90**, 75 (1997).
4. E. S. Lander, D. Botstein, *Genetics* **121**, 185 (1989).
5. J. van Rie, W. H. McGaughey, D. E. Johnson, B. D. Barnett, H. van Mellaert, *Science* **247**, 72 (1990).
6. J. Ferré, M. D. Real, J. van Rie, S. Jansens, M. Peferoen, *Proc. Natl. Acad. Sci. U.S.A.* **88**, 5119 (1991).
7. K. Luo *et al.*, *Insect Biochem. Mol. Biol.* **27**, 735 (1997).
8. S. S. Gill, E. A. Cowles, V. Francis, *J. Biol. Chem.* **270**, 27277 (1995).
9. S. T. Suzuki, *J. Cell. Biochem.* **61**, 531 (1996).
10. R. Vadlamudi, E. Weber, I. Ji, T. Ji, L. Bulla, *J. Biol. Chem.* **270**, 5490 (1995).
11. Y. Nagamatsu, T. Koike, K. Sasaki, A. Yoshimoto, Y. Furukawa, *FEBS Lett.* **460**, 385 (1999).
12. I. Arkhipova, N. Lyubomirskaya, Y. Ilyin, *Drosophila Retrotransposons* (Springer-Verlag, New York, 1995).
13. S. Marillonnet, S. R. Wessler, *Genetics* **150**, 1245 (1998).
14. T. Uemura, *Cell* **93**, 1095 (1998).
15. F. Gould *et al.*, *Proc. Natl. Acad. Sci. U.S.A.* **94**, 3519 (1997).
16. E. S. Lander *et al.*, *Genomics* **1**, 174 (1987).
17. A. Paterson *et al.*, *Nature* **335**, 721 (1988).
18. GenBank accession numbers AF367362 and AF367363. Prediction methods and alignment with BTR1 and BtR175 are documented in supplementary material available at *Science* Online (www.sciencemag.org/cgi/content/full/293/5531/857/DC1).
19. We thank A. Westman, D. Bourguet, and C. Robin for helpful comments on the manuscript. Supported by NSF grant MCB-9816056.

22 March 2001; accepted 15 June 2001

Bt Toxin Resistance from Loss of a Putative Carbohydrate-Modifying Enzyme

Joel S. Griffitts, Johanna L. Whitacre, Daniel E. Stevens, Raffi V. Aroian*

The development of resistance is the main threat to the long-term use of toxins from *Bacillus thuringiensis* (Bt) in transgenic plants. Here we report the cloning of a Bt toxin resistance gene, *Caenorhabditis elegans bre-5*, which encodes a putative β-1,3-galactosyltransferase. Lack of *bre-5* in the intestine led to resistance to the Bt toxin Cry5B. Wild-type but not *bre-5* mutant animals were found to uptake toxin into their gut cells, consistent with *bre-5* mutants lacking toxin-binding sites on their apical gut. *bre-5* mutants displayed resistance to Cry14A, a Bt toxin lethal to both nematodes and insects; this indicates that resistance by loss of carbohydrate modification is relevant to multiple Bt toxins.

Crystal toxins produced by *B. thuringiensis* are used worldwide in transgenic crops to control caterpillars and beetles, are an important tool of organic farming, and have made important contributions to the control of insect-borne diseases such as African river blindness. Once ingested by an insect, Bt toxins are proteolytically activated in the midgut and bind to membrane gut receptors, leading to pore formation and death (*1, 2*). Although Bt toxins are safe to vertebrates and are considered beneficial to the environment relative to chemical pesticides, Bt toxin effectiveness is threatened in the long term by the development of insect resistance (*3*). Bt-resistant variants of the diamondback moth have been identified in the field, and resistant strains of at least 11 insect species have been documented in the laboratory (*4, 5*). Understanding the molecular mechanism of toxin action and identifying the genes that can mu-

Section of Cell and Developmental Biology, University of California, San Diego, La Jolla, CA 92093, USA.

*To whom correspondence should be addressed. E-mail: raroian@ucsd.edu

tate to yield resistance are important steps in developing strategies to help delay or circumvent this problem.

Some Bt toxins are toxic to the nematode *C. elegans* (*6*). The best characterized of these nematicidal toxins, Cry5B, falls into a phylogenetic group of eight Bt toxins, at least two of which, Cry5A and Cry14A, are toxic to insects (*2*). Cry5B has ~24% sequence identity to commercially important insecticidal toxins, such as Cry1Ac, in the toxin domain. Cry5B contains four of the five protein sequence blocks conserved among most Bt toxins and may fold into a three-domain structure related to those of insecticidal toxins (*1, 7*). Like insects, nematodes fed Bt toxin rapidly cease feeding and incur intestinal damage (*6, 8*). These similarities in toxin sequences and response suggest that the general mechanism of Bt toxicity in nematodes and insects is conserved. By studying the process in *C. elegans*, we can take advantage of the molecular, genetic, and cell biological tools available in this model organism. In addition, nematicidal Bt toxins are important to study because of their potential to control plant-parasitic nematodes. These widespread

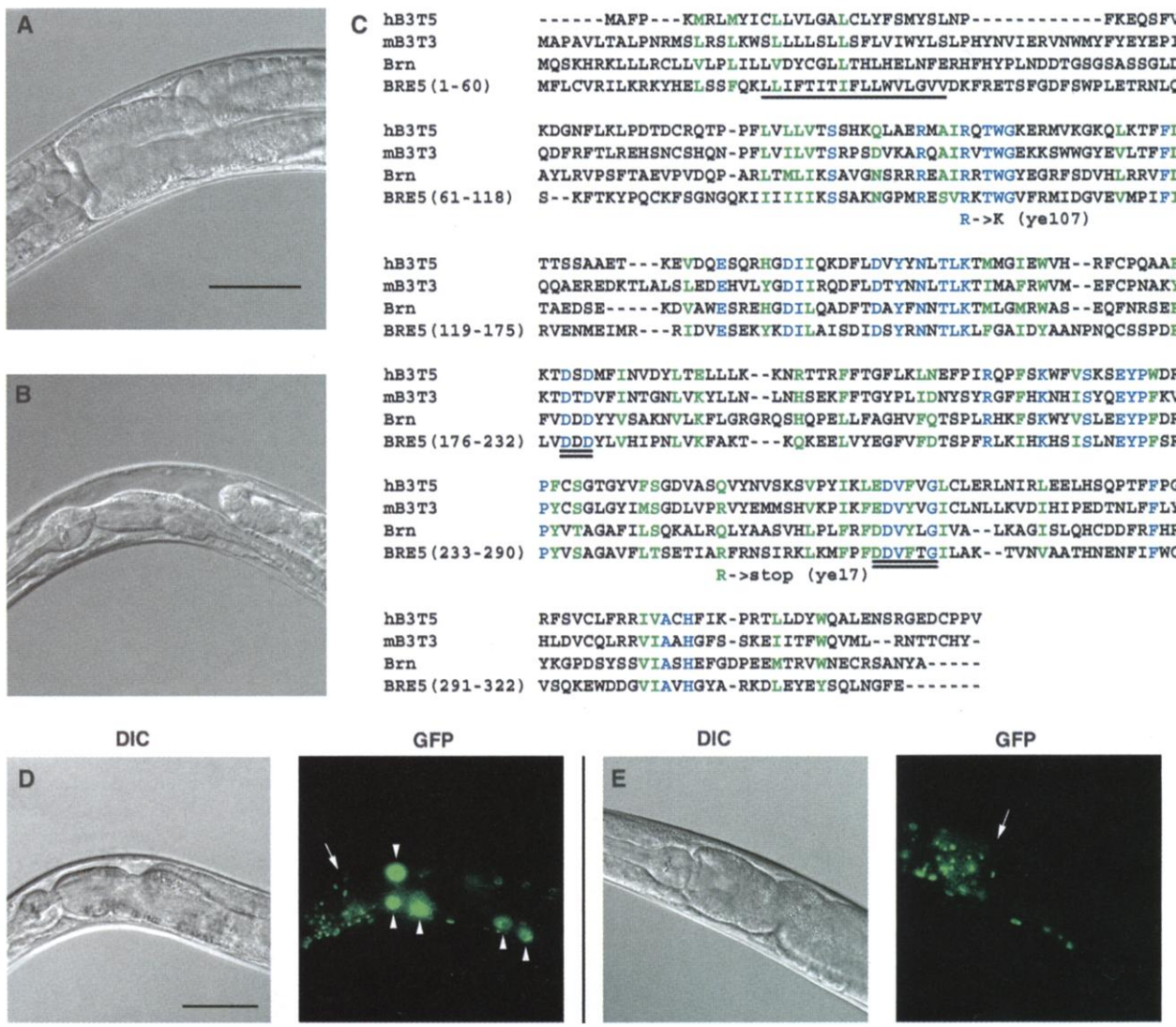

Fig. 1. BRE-5 encodes a putative galactosyltransferase that is required in the *C. elegans* gut for Bt toxin action. (**A** and **B**) Rescue experiments. In (A), a *bre-5(ye17)* animal fed Bt toxin for 24 hours shows a healthy, resistant gut. In (B), a *bre-5(ye17)* animal transformed with the 4.3-kb rescuing fragment fed Bt toxin for 24 hours shows a damaged, susceptible gut. Anterior is to the left. The posterior pharynx and anterior intestine are shown for each animal. Scale bar, 50 μm. (**C**) CLUSTALW (version 1.81) alignment of BRE-5 protein with human β-1,3-galactosyltransferase polypeptide 5 (hB3T5), mouse β-1,3-galactosyltransferase polypeptide 3 (mB3T3), and *Drosophila* BRAINIAC (Brn). Blue, absolutely conserved residues; green, conserved amino acid groups. The putative transmembrane domain is underlined; the DXD and DDVFTG motifs are double-underlined (single-letter abbreviations for amino acid residues: A, Ala; C, Cys; D, Asp; E, Glu; F, Phe; G, Gly; H, His; I, Ile; K, Lys; L, Leu; M, Met; N, Asn; P, Pro; Q, Gln; R, Arg; S, Ser; T, Thr; V, Val; W, Trp; and Y, Tyr). The locations of the two arginines mutated in the *bre-5* alleles are indicated: *ye107* alters an arginine conserved in all β-1,3-galatcosyltransferases; *ye17* introduces a premature stop codon. (**D** and **E**) Mosaic analysis showing that lack of BRE-5 in the gut leads to resistance to Bt toxin. Orientations are as in (A) and (B); scale bar, 50 μm. Arrows point to the anterior end of the gut. Exposures were identical for each pair of wild-type and *bre-5(ye17)* images. Shown in (D) are differential interference contrast (DIC) and deconvolved fluorescein isothiocyanate (FITC)–channel images of a *bre-5(ye17)* animal transformed with the extrachromosomal array that contains the 4.3-kb rescuing fragment (the animal is therefore sensitive to toxin) and SUR-5GFP(NLS), which results in GFP expression in the nuclei. Five large gut nuclei are in focus and brightly express GFP (arrowheads). In (E), DIC and deconvolved FITC-channel images of a mosaic animal that expressed GFP in some cells (and therefore contained the array) but was resistant to toxin (and therefore had lost the array in cells required for toxicity) are shown. In all 67 resistant animals, the gut nuclei never express GFP, indicating that the array was lost in the gut lineage. In the animal shown, the array is present in pharyngeal terminal bulb cells, descendants of the MS lineage.

agricultural pests cause ~$80 billion per year in crop damage (*9*) that is likely to be exacerbated by an upcoming worldwide ban of methyl bromide, the main chemical currently used to control them.

We previously reported the identification of five *C. elegans* genes, called *bre* (for Bt resistance), that mutate to Cry5B resistance (*6*). One of these genes, *bre-5*, was mapped to the right end of the chromosome IV cluster. We transformed *bre-5* mutant animals with cosmids in this area and rescued toxin resistance to toxin susceptibility in these animals with the cosmid T12G3 (*10*). We then narrowed down *bre-5* rescue to a 4.3-kb fragment within T12G3 (Fig. 1, A and B). This fragment did not contain any genes predicted in the genome database, but it did contain a single potential gene with extensive sequence similarity to mammalian glycosyltransferases. The cDNAs corresponding to this gene were isolated and a complete sequence assembled (*11*); it encodes a 322–amino acid protein (Fig. 1C). To confirm that this gene is *bre-5*, we sequenced the complete *bre-5* coding region from each of our two *bre-5* mutant alleles. Both alleles show alterations in this gene consistent with a loss or reduction of function (Fig. 1C).

BLAST and protein domain searches indicated that BRE-5 is a member of the β-1,3-galactosyltransferase family that transfers galactose onto proteins and lipids (*12*). BRE-5 is most similar in sequence to the *Drosophila* protein BRAINIAC. Over a 200–amino acid stretch that includes the catalytic domain, BRE-5 shows 37%, 27%, and 25% sequence identity to BRAINIAC, mouse β-1,3-galactosyltransferase 3, and human β-1,3-galactosyltransferase 5, respectively (Fig. 1C). BRAINIAC has been implicated in Notch signaling, perhaps by influencing ligand-receptor interactions, as has been speculated (*13, 14*). BRE-5 contains all the hallmarks of β-1,3-galactosyltransferases, including a putative NH_2-terminal transmembrane domain, an Asp-X-Asp motif, and a conserved variant of the Glu-Asp-Val-Tyr-Val-Gly motif. To confirm that loss of this galactosyltransferase gene leads to Bt toxin resistance, we injected hermaphrodite gonads with double-stranded (ds) RNA derived from the *bre-5* cDNA (*15*). Injection of dsRNA is known to deplete gene function in the progeny of injected hermaphrodites via RNA interference (RNAi) (*16*). After injections of dsRNA at 1.5 and 3.0 mg/ml, we found that, respectively, 45% (n = 60) and 73% (n = 60) of the progeny were resistant to Cry5B. These results confirm that Bt toxin resistance is the *bre-5* loss-of-function phenotype. As previously reported for *bre-5(ye17)* (*6*), we did not detect lethality or other obvious phenotypes in *bre-5* RNAi animals.

On the basis of the identification of BRE-5 as a putative galactosyltransferase and numerous in vitro studies that pointed to the importance of carbohydrates in the binding of insecticidal Cry1Ac to receptor and membrane (*17, 18*), we hypothesized that BRE-5 functions in forming a carbohydrate structure, present on proteins or lipids exposed at the gut surface, that is necessary for toxin binding. In the absence of *bre-5*–dependent carbohydrates, Bt toxin cannot bind, resulting in resistance. Such a requirement for carbohydrates in microbial toxin recognition would not be without precedent. For example, cholera toxin binds to host cells via carbohydrates (*19*).

To understand BRE-5 function better, we performed experiments involving mosaic animals to determine the anatomical focus of the gene's function with respect to Bt toxin susceptibility. Homozygous *bre-5(ye17)* hermaphrodites were injected with a cocktail of plasmids that included the dominant *rol-6* marker (which causes animals to roll), SUR-5GFP(NLS) [which is expressed in the nuclei of many somatic cells, including the intestine (*20*)], and the 4.3-kb rescuing fragment of *bre-5*. A stable line was established that transmitted all three transgenes as an extrachromosomal array in 50% of the progeny. As a result of *bre-5* rescue and expression of SUR-5GFP, rolling worms were sensitive to Cry5B, as expected, and displayed nuclear green fluorescent protein (GFP) (Fig. 1D). Of 2060 worms that were rolling (and therefore carrying the array) and were transferred to toxin plates, 67 rare, toxin-resistant animals were identified. These animals were resistant presumably because the extrachromosomal array had been lost during somatic divisions (*20*) in the tissue(s) where BRE-5 expression is needed for toxin to be effective. When these resistant, mosaic animals were examined for fluorescence, all 67 had lost GFP signal in the gut (Fig. 1E), indicating that the array and BRE-5 function were missing in the gut lineage, derived exclusively from the E blastomere. Furthermore, in 19 of these 67 animals, GFP staining still was present in posterior pharyngeal cells derived from MS, the sister of E (Fig. 1E), excluding the possibility that the array also had to be lost in other cells leading up to the birth of the E cell. We have verified that nonrolling mosaic animals also lack GFP fluorescence in the gut (20 of 20 animals). Thus, loss of the wild-type *bre-5* gene in the gut causes animals to be resistant to toxin. Consistent with this finding, we have performed immunofluorescence with a recently purified BRE-5 antibody that indicates expression in the gut (*21*).

To test directly whether BRE-5 is required for toxin to interact with the nematode gut in vivo, we fed fluorescently labeled Bt toxin to L4-staged hermaphrodites and followed its fate in wild-type and *bre-5* mutant animals (*22*). In wild-type animals, labeled toxin was internalized by gut cells, where it colocalized with autofluorescent gut granules, probably the site of the intestinal lysosome (*23*) (Fig. 2,

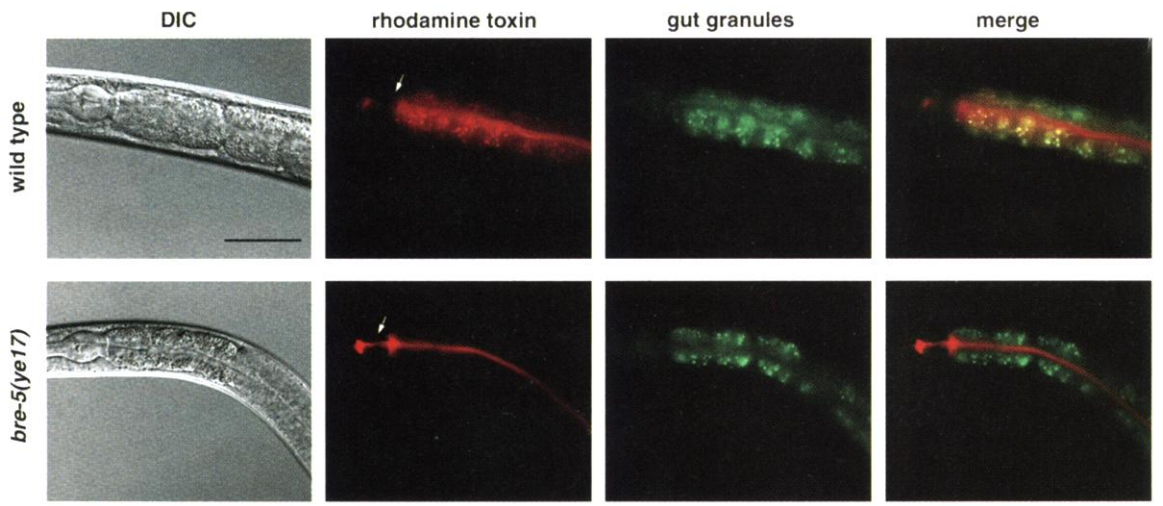

Fig. 2. *bre-5* mutant animals are defective in internalizing Bt toxin into gut cells. Wild-type and *bre-5(ye17)* animals were fed rhodamine-labeled Cry5B toxin for 1.5 hours and then imaged with DIC, in the rhodamine channel to visualize toxin, and in the FITC channel to visualize autofluorescent gut granules. Toxin was detected inside the wild-type gut cells and often colocalized with lysosomal gut granules. Toxin was not detected inside the *bre-5* mutant gut cells but was confined to the lumen. Anterior is to the left in each panel; arrows point to the anterior end of the gut. Exposures are identical for each pair of wild-type and *bre-5(ye17)* images.

upper panels). This uptake into wild-type gut cells was seen as rapidly as 20 min after feeding was initiated. These data suggest that toxin binds to the nematode gut via receptors and is then endocytosed. In contrast, when *bre-5(ye17)* animals were fed labeled toxin, toxin remained in the intestinal lumen and was not internalized by gut cells (Fig. 2, lower panels).

To rule out the possibility that the *bre-5* mutant gut was generally defective in endocytosis, we fed wild-type and *bre-5(ye17)* animals the lipophilic dye FM4-64, a marker for membrane-mediated endocytosis, and rhodamine-labeled bovine serum albumin (BSA), a marker for fluid-phase endocytosis. Within 20 min, FM4-64 dye entered gut cells and colocalized with lysosomal gut granules in both wild-type and mutant animals, with indistinguishable kinetics. Rhodamine-BSA also entered wild-type and mutant gut cells with similar kinetics, but took much longer to detect than did FM4-64 or toxin. These data indicate that membrane-mediated and fluid-phase endocytosis occur relatively normally in the *bre-5* mutant. Moreover, the finding that the rapid uptake of toxin into gut cells more closely resembles uptake of FM4-64 than that of rhodamine-BSA is consistent with toxin entering gut cells by membrane association rather than by fluid-phase endocytosis.

We have also ruled out the idea that *bre-5* mutant animals have altered feeding behaviors that might affect the ability of toxin to interact with the gut membrane. We found that pharyngeal pumping rate (243 ± 9 pumps per min in wild type, 242 ± 11 in *bre-5(ye17)*; $n = 10$ for both) and defecation rate (48 ± 5 s per cycle in wild type, 49 ± 7 s per cycle in *bre-5(ye17)*; $n = 10$ for both) are not affected in the *bre-5* mutant.

To address how widespread the *bre-5* resistance mechanism might be, we tested whether *bre-5* mutants were resistant to other Bt toxins. We took advantage of the fact that there is a known Bt toxin, Cry14A, that is part of the same phylogenetic subgroup of Bt toxins as Cry5B and is toxic to both nematodes and insects (*2, 24, 25*). Cry14A is 23% identical to Cry1Ac and 34% identical to Cry5B in the toxin domain. As with Cry5B, wild-type *C. elegans* fed Cry14A rapidly show gut damage. We found that *bre-5(ye17)* animals were sick on plates expressing high levels of Cry14A but were healthy on plates expressing lower levels of Cry14A that were still toxic to wild-type animals. To quantitate this dose-dependent resistance, we performed brood size assays for wild-type and *bre-5(ye17)* animals in the presence of variable amounts of Cry14A toxin (Fig. 3) (*26*). These data indicate that, relative to the wild type, *bre-5(ye17)* is 19 times as resistant to Cry14A.

Because *bre-5* mutants show resistance to two divergent Bt toxins that share only 34% identity, this mechanism of resistance is likely to be applicable to other Bt toxins as well. Our Cry14A data also suggest that this mechanism is relevant for insects, because Cry14A is toxic to the beetle *Diabrotica* spp. It is likely that Cry14A recognizes the same carbohydrate structure in the beetle as in the nematode, and that *bre-5*–mediated resistance could develop in this insect with this toxin.

Our identification and characterization of *bre-5* as a Bt resistance gene provides evidence in vivo for the importance of carbohydrates in Bt toxicity and the development of resistance. It is noteworthy that in the commercially important insecticidal toxins Cry1Aa and Cry3A, subdomain II folds into a β prism structure similar to that found in the plant lectins jacalin and *Maclura pomifera* agglutinin (*27, 28*). Both of these lectins are highly specific for binding the carbohydrate galactose β-1,3-*N*-acetylgalactosamine, precisely the type of structure made by the BRE-5 family of enzymes. Thus, it is conceivable that the binding of these insecticidal toxins requires a carbohydrate structure similar to that putatively formed by BRE-5.

Our results potentially explain a dilemma in the Bt field, namely that a single toxin can bind to at least two receptors that are completely unrelated in sequence (*2*). We hypothesize that these disparate receptors are able to bind the same toxin through a common carbohydrate motif. Resistance by loss of a carbohydrate-modifying enzyme is thus particularly dangerous and more threatening than mutation of a single receptor. Loss of a single general modifier such as BRE-5 could affect the binding of multiple Bt toxins to multiple receptors, leading to a high level of resistance to a single toxin and cross-resistance to other toxins as well. Determining how widespread this type of resistance is among different invertebrates—and how to deal with it—is vital for the long-term effectiveness of this important technology.

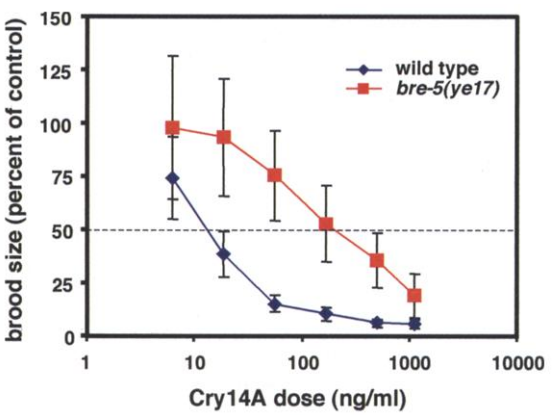

Fig. 3. Relative to the wild type, *bre-5(ye17)* is 19 times as resistant to Cry14A. The 3-day brood sizes of wild-type and *bre-5* animals were counted in varying doses of Cry14A toxin. Percent of control indicates the percent progeny relative to the 3-day brood sizes of wild-type and *bre-5(ye17)* in the absence of toxin, which are 132 ± 38 and 99.2 ± 28, respectively. The dose at which their brood sizes are reduced to 50% is 11.2 ng/ml in wild-type and 210 ng/ml in *bre-5(ye17)*.

References and Notes

1. E. Schnepf *et al.*, *Microbiol. Mol. Biol. Rev.* **62**, 775 (1998).
2. R. A. de Maagd, A. Bravo, N. Crickmore, *Trends Genet.* **17**, 193 (2001).
3. F. Gould, *Annu. Rev. Entomol.* **43**, 701 (1998).
4. B. E. Tabashnik, *Proc. R. Soc. London Ser. B* **255**, 7 (1994).
5. W. H. McGaughey, B. Oppert, *Isr. J. Entomol.* **2**, 1 (1998).
6. L. D. Marroquin, D. Elyassnia, J. S. Griffitts, J. S. Feitelson, R. V. Aroian, *Genetics* **155**, 1693 (2000).
7. N. Crickmore *et al.*, *Microbiol. Mol. Biol. Rev.* **62**, 807 (1998).
8. J. S. Griffitts, R. V. Aroian, unpublished data.
9. J. N. Sasser, D. W. Freckman, in *Vistas on Nematology: A Commemoration of the Twenty-Fifth Anniversary of the Society of Nematologists*, J. A. Veech, D. W. Dickson, Eds. (Society of Nematologists, Hyattsville, MD, 1987), pp. 7–14.
10. We injected *bre-5(ye17)* (*6*) hermaphrodites with a DNA cocktail containing the cosmid T12G3 (10 ng/μl) and plasmid pRF4 (80 ng/μl), which expresses a dominant *rol-6* gene. Two of three stably transformed lines showed robust rescue. The 4.3-kb rescuing fragment was made by polymerase chain reaction (PCR) amplification with a mixture of Taq and Pfu polymerases using T12G3 and primers 5′-GGCTCTAGACACCAACTCTCCAGCTTTC-3′ and 5′-GATATGCAAATTCGATTCGTCATG-3′ and subcloning of the resulting 4.3-kb piece into pBluescript. When this plasmid was injected at 10 ng/μl along with pRF4 at 50 ng/μl, robust F_1 and F_2 rescue (2 of 2 lines) was seen. The *ye107* allele was isolated in a genetic screen for animals resistant to *Escherichia coli*–expressed Cry5B (*6*); *ye107* fails to complement *bre-5(ye17)* but complements alleles of the other four *bre* genes (L. Marroquin, R. V. Aroian, unpublished data).
11. For cDNA cloning, see supplementary material at *Science* Online (www.sciencemag.org/cgi/content/full/293/5531/860/DC1).
12. M. Amado, R. Almeida, T. Schwientek, H. Clausen, *Biochim. Biophys. Acta* **1473**, 35 (1999).
13. K. Bruckner, L. Perez, H. Clausen, S. Cohen, *Nature* **406**, 411 (2000).
14. V. M. Panin, K. D. Irvine, *Semin. Cell Dev. Biol.* **9**, 609 (1998).
15. The subclone that encodes the entire *bre-5* cDNA cloned into pBluescript was PCR-amplified by T3 and T7 primers. RNA was prepared and purified from this PCR product using Megascript T3 and T7 kits (Ambion), annealed, and injected into wild-type adults. After 16 to 24 hours, L1- to L3-staged progeny were transferred to plates spread with *E. coli* expressing Cry5B toxin and scored 24 and 48 hours later for resistance. We have confirmed that injection of unrelated dsRNAs does not lead to resistance.
16. R. H. A. Plasterk, R. F. Ketting, *Curr. Opin. Genet. Dev.* **10**, 562 (2000).
17. J. L. Jenkins, M. K. Lee, S. Sangadala, M. J. Adang, D. H. Dean, *FEBS Lett.* **462**, 373 (1999).
18. S. L. Burton, D. J. Ellar, J. Li, D. J. Derbyshire, *J. Mol. Biol.* **287**, 1011 (1999).
19. B. D. Spangler, *Microbiol. Rev.* **56**, 622 (1992).
20. J. Yochem, T. Gu, M. Han, *Genetics* **149**, 1323 (1998).
21. J. L. Whitacre, J. S. Griffitts, R. V. Aroian, unpublished data.
22. Cry5B crude spore lysate pellets (*6*) were resuspended with 3.8 ml of water and toxin crystals solubilized with 30 ml of acid solubilization buffer (8.7 mM

tripotassium citrate, 43.4 mM citric acid, and 10 mM dithiothreitol). Spores and insoluble material were spun out at 8000 rpm. Toxin was precipitated from the supernatant by adding 0.75 ml of 1 M tripotassium citrate and stored at −80°C. Toxin was solubilized by resuspending in 20 mM Hepes (pH 8.0) at a final concentration of 4 mg/ml. To test the quality of this purified toxin, we determined the concentration at which 50% of the animals die after exposure for 5 days at 20°C (LC_{50}) to be 16.7 μg/ml, similar to the 12.6 μg/ml reported for toxin present in crude spore lysates (*6*). Toxin was labeled in the presence of a fourfold molar excess of *N*-hydroxysuccinimide–rhodamine (Pierce 46102) and purified away from unincorporated rhodamine by gel filtration. Labeled toxin has potent but reduced toxicity (LC_{50} = 31.8 μg/ml). Feeding assays were performed with L4-staged hermaphrodites in wells containing egg salts with 100 mM glucose and labeled toxin (50 μg/ml), FM4-64 (20 μg/ml), or rhodamine-BSA (0.1 mg/ml). Images were collected on an Olympus IX-70 inverted microscope (40×, 1.35 NA objective) and a MicroMax camera (Roper Instruments).

23. M. Kostich, A. Fire, D. M. Fambrough, *J. Cell Sci.* **113**, 2595 (2000).
24. J. Payne, K. Narva, World Intellectual Property Organization Patent 94/16079 (1994).
25. _____, J. Fu, U.S. Patent 5,589,382 (1995).
26. As was done previously for Cry5B (*6*), DNA equivalent to the Cry14A coding sequence was cloned into the pQE9 expression vector and transformed into JM103 cells. Single L4-staged hermaphrodites were placed in 120-μl single-well assays that included S medium, antibiotics, and 10 μl of *E. coli* induced to express Cry14A and/or vector alone (*6*). The amount of toxin was quantitated by comparing the Cry14A band against BSA standards on SDS gels and was varied by altering the mixture of bacteria expressing either empty vector or Cry14A. The total optical density of bacteria added to the well was always constant. Brood sizes were counted after 3 days at 25°C. The data from the 19 animals were taken from two independent experiments. We repeated the experiments with *E. coli* expressing Cry5B and found that at a Cry5B concentration of 3.3 μg/ml, wild-type animals had a brood of 5.1 ± 3.3 progeny (n = 20), whereas *bre-5(ye17)* animals had a brood of 99 ± 28 progeny (n = 20, compared to 104 ± 36 progeny without toxin).
27. X. Lee *et al.*, *J. Biol. Chem.* **273**, 6312 (1998).
28. R. Sankaranarayanan *et al.*, *Nature Struct. Biol.* **3**, 596 (1996).

29. We thank L. Marroquin for information that helped in the cloning of *bre-5*, B. Grant for help with endocytosis assays, J. Posakony and B. Oppert for critical reading of the manuscript, J. Esko and members of the Aroian laboratory for helpful discussions, and T. Stiernagle at the *C. elegans* Genetics Center (funded by the NIH National Center for Research Resources) for *C. elegans* stocks. Supported by NSF grant MCB-9983013 (R.V.A.), a Burroughs Wellcome New Investigators Award in Toxicological Sciences, and a Beckman Foundation Young Investigators Award. The GenBank accession number for *bre-5* sequence is AY038065.

10 May 2001; accepted 15 June 2001

Myotonic Dystrophy Type 2 Caused by a CCTG Expansion in Intron 1 of *ZNF9*

Christina L. Liquori,[1,2] Kenneth Ricker,[4] Melinda L. Moseley,[1,2] Jennifer F. Jacobsen,[1,2] Wolfram Kress,[5] Susan L. Naylor,[6] John W. Day,[1,3]* Laura P. W. Ranum[1,2]*

Myotonic dystrophy (DM), the most common form of muscular dystrophy in adults, can be caused by a mutation on either chromosome 19q13 (DM1) or 3q21 (DM2/PROMM). DM1 is caused by a CTG expansion in the 3′ untranslated region of the dystrophia myotonica–protein kinase gene (*DMPK*). Several mechanisms have been invoked to explain how this mutation, which does not alter the protein-coding portion of a gene, causes the specific constellation of clinical features characteristic of DM. We now report that DM2 is caused by a CCTG expansion (mean ~5000 repeats) located in intron 1 of the zinc finger protein 9 (*ZNF9*) gene. Parallels between these mutations indicate that microsatellite expansions in RNA can be pathogenic and cause the multisystemic features of DM1 and DM2.

DM is a dominantly inherited, multisystemic disease with a consistent constellation of seemingly unrelated and rare clinical features including myotonia, muscular dystrophy, cardiac conduction defects, posterior iridescent cataracts, and endocrine disorders (*1*). DM was first described nearly 100 years ago (*2*), but the existence of more than one genetic cause was only recognized after genetic testing became available for myotonic dystrophy type 1 (DM1) (*3, 4*).

DM1 is caused by an expanded CTG repeat on chromosome 19 that is both in the 3′ untranslated region of the dystrophia myotonica–protein kinase (*DMPK*) gene, and in the promoter region of the immediately adjacent homeodomain gene *SIX5* (*5, 6*). How the CTG expansion in a noncoding region of a gene causes the complex DM phenotype remains unclear (*5, 6*). Suggested mechanisms include: (i) haploinsufficiency of the dystrophia myotonica–protein kinase (DMPK) protein (*7*); (ii) altered expression of neighboring genes, including *SIX5* (*8–12*); and (iii) pathogenic effects of the CUG expansion in RNA which accumulates as nuclear foci (*13, 14*) and disrupts cellular function (*15–18*). Several mouse models have developed different aspects of DM1: a model expressing mRNA with CUG repeats manifests myotonia and the myopathic features of DM1 (*19*); a *DMPK* knockout has cardiac abnormalities (*20*); and *SIX5* knockouts have cataracts (*21, 22*). Taken together, these data have been interpreted to suggest that each theory may contribute to DM1 pathogenesis and that DM1 may be a regional gene disorder (*5, 6*).

Defining a second human mutation that causes the multisystemic effects of DM, and identifying what is common to these diseases at the molecular level, provides an independent means of determining the pathogenic pathway of DM. Toward this goal, we mapped the myotonic dystrophy type 2 [DM2/proximal myotonic myopathy (PROMM)] locus to chromosome 3q21 (*23, 24*) and have used positional cloning to identify the DM2 mutation.

The DM2 region was narrowed to a 2-cM interval (*25*) by analyzing 10 recombinant chromosomes (*25*). Sequence data (*26, 27*) from this region, which is partially covered by 14 bacterial artificial chromosomes (BACs), was used to develop 80 short tandem repeat (STR) markers. Linkage disequilibrium analysis (*27*) was performed on 64 parent-offspring trios in which affected individuals had the clinical features of DM but not the DM1 mutation. Transmission disequilibrium testing (*28*) and analysis of conserved ancestral haplotypes narrowed the DM2 locus to a region of ~320 kilobases (kb) (Fig. 1A).

One of the markers in linkage disequilibrium with DM2, *CL3N58* ($P \leq 0.000001$), showed an aberrant segregation pattern. All affected individuals appeared to be homozygous by polymerase chain reaction (PCR) (*29*), and affected children appeared not to inherit an allele from their affected parent (Fig. 1, B and C). Southern (DNA) analysis was performed (*30*) to investigate the possibility that the aberrant segregation pattern was caused by a repeat expansion or other rearrangement. In addition to the expected normal allele, we detected a variably sized expanded allele, too large to amplify by PCR, that was found only in affected individuals (Fig. 1, B and D). Modified electrophoresis conditions

[1]Institute of Human Genetics; [2]Department of Genetics, Cell Biology, and Development; and [3]Department of Neurology MMC 206, 420 Delaware Street SE, University of Minnesota, Minneapolis, MN 55455, USA. [4]Department of Neurology and [5]Institute of Human Genetics, University of Würzburg, Germany. [6]Department of Cellular and Structural Biology, University of Texas Health Science Center at San Antonio, San Antonio, TX 78284, USA.

*To whom correspondence should be addressed. E-mail: johnday@umn.edu (J.W.D.); ranum001@umn.edu (L.P.W.R.).